

# Continuum Double Exchange Model

*José María Román and Joan Soto*

*Departament d'Estructura i Constituents de la Matèria*

*and*

*Institut de Física d'Altes Energies*

*Universitat de Barcelona*

*Diagonal, 647*

*E-08028 Barcelona, Catalonia, Spain.*

*e-mails:* roman@ecm.ub.es, soto@ecm.ub.es

December 2, 2024

## Abstract

We present a continuum model for doped manganites which consist of two species of quantum spin 1/2 fermions interacting with classical spin fields. The phase structure at zero temperature turns out to be considerably rich: antiferromagnetic insulator, antiferromagnetic two band conducting, canted two band conducting, canted one band conducting and ferromagnetic one band conducting phases are identified, all of them being stable against phase separation. There are also regions in the phase diagram where phase separation occurs.

PACS: 75.30.Et, 75.25.+z, 11.30.Qc, 75.10.-b

# 1 Introduction

Doped manganites  $La_{1-x}A_xMnO_3$  ( $A$  divalent) [1] are receiving quite a lot of both theoretical [2, 3, 4, 5, 6, 7, 8, 9] and experimental [10] attention lately. These materials show an interesting interplay between magnetism and conductivity with intrincated phase diagrams which are still controversial.

In a cubic lattice the  $3d$  orbitals of  $Mn$  split into a  $t_{2g}$  triplet and an upper  $e_g$  doublet. Due to the electronic repulsion and the Fermi statistics (Hund's rule) the three  $t_{2g}$  levels are always single occupied forming a core  $S = 3/2$  spin. The  $e_g$  orbitals may be further splitted by a static Jahn-Teller distortion at small doping [11].

The above features are encoded in the so called double exchange models of different degrees of complexity. The simpler ones assume a strong Jahn-Teller distortion so that only the lower  $e_g$  level is consider. Hence there is a single fermion field in each site, with a spin independent hopping term and a local interaction with the core spin [4, 5]. Core spins also interact among themselves with the usual Heisenberg term. Under certain assumptions [12] the interaction with the core spin can be traded for an angle dependent hopping term [2, 13]. The next level of complexity consist of taking into account the two  $e_g$  levels [6, 7], and only very recently, the Jahn-Teller distortion has been incorporated dynamically by some authors [9].

It is the aim of this work to present a simple continuum model for doped manganites which also encodes the basic features above and, moreover, is exactly solvable for classical core spins. It produces a rich phase diagram which is in qualitative agreement with recent results and it shows, in addition, that stable canted phases exist. The main advantage with respect to previous approaches is that all the parameters of the material (lattice spacing, band curvature, Hund coupling, Heisenberg coupling and doping) combine into only two constants. This allows to present a two dimensional phase diagram which holds for a large amount of materials.

## 2 The Model

Cooperative phenomena are amenable of a field theoretical description. When the phenomena do not depend on the details of the microscopic system but only on its long wave length behaviour a continuum field theory description is appropriated. The field theoretical continuum model must contain the relevant degrees of freedom at long wavelengths, which depend on the particular systems and phenomena that are to be studied. In our case, these are doped manganites and their phase diagram at zero temperature. These systems

are known to undergo a number of phase transitions when the doping is increased. They are insulating antiferromagnets (*AFI*) at zero doping and become conducting ferromagnets (*FC*) at large enough doping. What happens between these two regimes is still controversial, though most of authors agree that the phase diagram is very rich and non-trivial. Early works on the subject suggested that an interesting intermediate conducting canted phase exists [13], but recent experimental [10] and theoretical [2, 4] results indicate that the canted phase appears to be unstable against phase separation.

Theoretical work on the subject is based on variations of the double exchange models. The phase structure of the system is obtained from these models using certain simplifying assumptions (slave boson formalism [2], trial wave functions [4],...) or extensive numerical simulations [9], the scope of which is difficult to evaluate. We present below a continuum field theoretical model which, as we shall argue, contains the relevant long wavelength degrees of freedom of the system. Then our main assumption is going to be that the rich phase diagram of manganites can be understood from long wavelength physics only. As the model is exactly solvable, there are no further uncertainties due to uncontrolled approximations.

Since we wish our model to include the well established *AFI* and *FC* phases, we need at least an *AF* order parameter field, a *F* order parameter field, and a *I – C* order parameter field. For the *AF* and *F* order parameter fields we shall use  $\mathbf{M}_1(x)$  and  $\mathbf{M}_2(x)$  the local magnetisations in the even and odd sublattices respectively. Both in the *AF* and *F* phases these local magnetisations are smoothly varying fields. In the *AF* phase  $\mathbf{M}_1(x)\mathbf{M}_2(x) \sim -1$  whereas in the *F* phase  $\mathbf{M}_1(x)\mathbf{M}_2(x) \sim 1$ . For the *I – C* order parameter one could think of introducing a single slowly varying spin 1/2 fermion field together with a chemical potential which regulates the doping. When the chemical potential is below the energy gap of the lowest spin state we have an *I* phase, when it overtakes this energy gap we have a one band *C* phase, and when it overtakes the energy gap of the highest spin state we have a two band *C* phase. However, a spin 1/2 field naturally couples to the local magnetisation, which changes abruptly from the even to the odd sublattice in the *AF* phase. Hence in this phase a single spin 1/2 field cannot be slowly varying over the system. We need at least two slowly varying spin 1/2 fermionic fields,  $\psi_1(x)$  which couples to the magnetisation in the even sublattice  $\mathbf{M}_1(x)$  and  $\psi_2(x)$  which couples to the magnetisation in the odd sublattice  $\mathbf{M}_2(x)$ . Since the conductivity is due to fermions moving from one sublattice to the other one a (spin independent) hopping term is introduced. The allowed values of the chemical potential will be limited by the physical condition that no conduction must exist when the hopping parameter vanishes.

The model must be *SU*(2) spin invariant since the magnetic interactions emerge from the usual superexchange mechanism together with the Hund's rule. The space-time symmetries

of the underlying crystal must also be implemented and will be the only remain of the microscopic lattice structure. For simplicity we shall take a cubic lattice and comment later on the slight modifications that occur for other crystals.

The lagrangian of the model reads

$$\begin{aligned}\mathcal{L}(x) = & \psi_1^\dagger(x) \left[ (1 + i\epsilon)i\partial_0 + \frac{\partial_i^2}{2m} + \mu + J_H \frac{\boldsymbol{\sigma}}{2} \mathbf{M}_1(x) \right] \psi_1(x) \\ & + \psi_2^\dagger(x) \left[ (1 + i\epsilon)i\partial_0 + \frac{\partial_i^2}{2m} + \mu + J_H \frac{\boldsymbol{\sigma}}{2} \mathbf{M}_2(x) \right] \psi_2(x) \\ & + t \left( \psi_1^\dagger(x) \psi_2(x) + \psi_2^\dagger(x) \psi_1(x) \right) - J_{AF} \mathbf{M}_1(x) \mathbf{M}_2(x).\end{aligned}\quad (2.1)$$

The size of the parameters in the model are estimated by comparing them with the naïve continuum limit of lattice double exchange models. For a cubic lattice we have  $2m \sim 1/a^2 t^l$ ,  $t \sim z t^l$ ,  $J_H \sim J_H^l$  and  $J_{AF} \sim z J_{AF}^l / a^3 > 0$ , where  $a$  is the lattice spacing,  $z = 6$  is the coordination number and the superscript  $l$  means the analogous lattice quantity. The fields  $\psi_i(x)$  may describe either electrons or holes. Since the conduction in actual doped manganites is due to holes, one should better figure out  $\psi_i(x)$  as hole annihilating fields. Recall that for holes  $J_H$  is negative whereas it is positive for electrons. This sign however is going to be irrelevant as far as the phase diagram is concerned.

The lagrangian above is invariant under the following transformations:

(i) Global  $SU(2)$  spin transformations,

$$\begin{aligned}\psi_i(x) & \longrightarrow g \psi_i(x) \\ M_i^a(x) & \longrightarrow R_b^a M_i^b(x),\end{aligned}\quad (i = 1, 2) \quad (2.2)$$

(ii) Primitive translations,

$$\begin{aligned}\psi_1(x) & \longrightarrow \psi_2(x) & \psi_2(x) & \longrightarrow \psi_1(x) \\ \mathbf{M}_1(x) & \longrightarrow \mathbf{M}_2(x) & \mathbf{M}_2(x) & \longrightarrow \mathbf{M}_1(x),\end{aligned}\quad (2.3)$$

(iii) Point group transformations, given by the group  $m\bar{3}m$

$$\begin{aligned}\psi_i(x) & \longrightarrow g_\xi \psi_i(\xi^{-1}x) \\ M_i^a(x) & \longrightarrow R_b^a(\xi) M_i^b(\xi^{-1}x)\end{aligned}\quad (i = 1, 2), \quad (2.4)$$

when the point group transformation  $\xi$  maps points in the same sublattice, and

$$\begin{aligned}\psi_1(x) & \longrightarrow g_\xi \psi_2(\xi^{-1}x) & \psi_2(x) & \longrightarrow g_\xi \psi_1(\xi^{-1}x) \\ M_1^a(x) & \longrightarrow R_b^a(\xi) M_2^b(\xi^{-1}x) & M_2^a(x) & \longrightarrow R_b^a(\xi) M_1^b(\xi^{-1}x),\end{aligned}\quad (2.5)$$

when the transformation  $\xi$  maps points of different sublattices. Anyway, the rotations  $g_\xi$  and  $R_b^a(\xi)$  can be absorbed by a  $SU(2)$  transformation and the change of sublattice in (2.5) by a primitive translation. Hence, in practice, we only have to care about the transformation of the coordinates.

(iv) Time reversal,

$$\begin{aligned}\psi_i(x) &\longrightarrow C\psi_i^*(Tx) \\ \mathbf{M}_i(x) &\longrightarrow -\mathbf{M}_i(Tx)\end{aligned}\quad C = e^{-i\pi\sigma^2/2} = -i\sigma^2 \quad , \quad (i = 1, 2), \quad (2.6)$$

where  $Tx = (-t, \mathbf{x})$ .

### 3 Effective Potential

In order to find out how the ground state of the system changes as a function of the chemical potential, we shall calculate the effective potential and minimise it with respect to the order parameters  $\mathbf{M}_1$  and  $\mathbf{M}_2$ . We shall assume that the ground state configuration corresponds to constant magnetisations both in the odd and even sublattices. Hence, the effective potential is to be minimised with respect to the angle  $\theta$  between  $\mathbf{M}_1$  and  $\mathbf{M}_2$  only. We use  $y = \cos(\theta/2)$ . When  $y = 0$ ,  $0 < y < 1$  and  $y = 1$  we have an antiferromagnetic, canted and ferromagnetic phase respectively.

The effective potential is obtained by integrating out the fermion fields in the path integral, and it is formally given by

$$V_{eff} = J_{AF}\mathbf{M}_1\mathbf{M}_2 + itr \log \hat{O}/VT, \quad (3.1)$$

where

$$\hat{O} = \begin{pmatrix} (1+i\epsilon)i\partial_0 + \partial_i^2/2m + \mu + \frac{J_H}{2}\boldsymbol{\sigma}\mathbf{M}_1 & t \\ t & (1+i\epsilon)i\partial_0 + \partial_i^2/2m + \mu + \frac{J_H}{2}\boldsymbol{\sigma}\mathbf{M}_2 \end{pmatrix}, \quad (3.2)$$

and the trace is both on spin indices and space-time coordinates.  $VT$  is the volume of the space-time.

If  $\hat{O}$  has eigenvalues  $\lambda_n$

$$tr \log \hat{O} = \sum_n \log \lambda_n. \quad (3.3)$$

We have then to diagonalise the operator  $\hat{O}$ . Since it contains only constant fields the diagonalisation with respect to the space-time is trivially attained by plane waves. The

diagonalisation with respect to the spin indices is a simple linear algebra problem. We obtain

$$\lambda_n = O_i(q) = (1 + i\epsilon) \omega - \frac{\mathbf{k}^2}{2m} - \Omega_i \quad (3.4)$$

$$\Omega_i = \pm \frac{|J_H|M}{2} \sqrt{1 + \gamma^2 \pm 2\gamma \cos \frac{\theta}{2}} - \mu \quad , \quad \gamma \equiv \frac{2t}{|J_H|M}. \quad (3.5)$$

$q = (\omega, \mathbf{k})$  and  $M = |\mathbf{M}_1| = |\mathbf{M}_2| = 3/2$ . The restriction for the values of the chemical potential in the model implies that at most the two lower eigenvalues in (3.5) may contribute. This motivates the following reparametrisation of the chemical potential:

$$\mu = -\frac{|J_H|M}{2} \sqrt{1 + \gamma^2 - 2\gamma y_0} \quad (-1 < y_0 < y_0^{max} = \gamma/2), \quad (3.6)$$

which eases comparison with the energy levels in (3.5) ( $y = \cos(\theta/2)$ ). In order to simplify the analysis we assume  $\gamma$  small and keep only linear terms in  $\gamma$  in the relevant eigenvalues above. Namely,

$$\Omega_i = -\frac{|J_H|M}{2} \gamma (y_0 \pm y). \quad (3.7)$$

This is justified for  $t \ll J_H$ , as it turns out to be the case for the actual materials [14]. Anyway, this simplification can be lifted with the only drawback that the few analytic expressions below must also be substituted by numerical analysis.

In order to calculate the sum (3.3) we have used  $\zeta$ -function techniques [15], which are explained in the appendix. We obtain the effective potential (for  $\mu < 0$ )

$$V_{eff} = V_0 \left[ (2y^2 - 1) - A \left( (y_0 + y)^{5/2} \theta(y_0 + y) + (y_0 - y)^{5/2} \theta(y_0 - y) \right) \right], \quad (3.8)$$

where we have defined

$$V_0 = J_{AF} M^2 \quad , \quad A = \frac{(2m)^{3/2} t^{5/2}}{15\pi^2 J_{AF} M^2} = \frac{z^{3/2}}{15\pi^2} \frac{t}{(J_{AF} a^3 M^2)}. \quad (3.9)$$

## 4 Phase Structure

The possible phases of the model are obtained by minimising (3.8) with respect to  $y$  for the different values of the parameters  $A$  and  $y_0$ . The number of conducting bands is given by the number of  $\theta$ -functions in (3.8) which contribute to the effective potential at the minimum.

In order to gain some qualitative understanding and to make the minimisation procedure systematic we shall first separate the cases  $y_0 < 0$  and  $y_0 > 0$ . For each case we shall work

out the stability conditions for  $AF$  ( $y = 0$ ), canted ( $0 < y < 1$ ) and  $F$  ( $x = 1$ ) phases. After that we shall compare the energy of the stable phases and obtain the curves which separate them.

The stability conditions are given for the different phases by

$$\begin{aligned} AF : \quad & V'_{eff}(0) > 0 \quad \text{or} \quad V'_{eff}(0) = 0 \quad V''_{eff}(0) > 0 \\ C : \quad & V'_{eff}(y_c) = 0 \quad V''_{eff}(y_c) > 0 \\ F : \quad & V'_{eff}(1) < 0. \end{aligned} \tag{4.1}$$

Let us then consider first the case  $y_0 < 0$ . Clearly for  $y_0 < -1$  the unique existing phase is the  $AFI$  phase. In the case  $-1 < y_0 < 0$  only the lowest of the four spin eigenvalues may contribute to the effective potential. The stability conditions yield the following stable phases:

$$\begin{aligned} AFI : \quad & y = 0 \\ FC : \quad & y = 1 \quad A(1 + y_0)^{3/2} > 8/5. \end{aligned} \tag{4.2}$$

The canted phase is not stable as it can be seen from the condition  $V'_{eff}(y_c) = 0$ ,

$$y_c = \frac{5}{8}A(y_0 + y_c)^{3/2}, \tag{4.3}$$

which has at most one solution  $y_c \in [-y_0, 1]$ . Since  $V_{eff}$  is continuous, and increasing at  $y = 0$  this solution must be a maximum when it exists.

The curve  $V_{eff}(0) = V_{eff}(1)$  in the plain  $(y_0, A)$ , which separates the  $AF$  and  $F$  phases, reads

$$A(1 + y_0)^{5/2} = 2 \quad (-1 < y_0 < 0). \tag{4.4}$$

Above this curve the  $F$  phase is favoured against the  $AF$  phase and viceversa.

Consider next the case  $0 < y_0 < 1$ . The stability conditions are given by

$$\begin{aligned} AFC2 : \quad & y = 0 \quad Ay_0^{1/2} < 8/15 \\ CC2 : \quad & 5A(y_c^2 + 3y_0^2)/4 = (y_0 + y_c)^{3/2} + (y_0 - y_c)^{3/2} \quad 8/15 < Ay_0^{1/2} < 2\sqrt{2}/5 \\ CC1 : \quad & y_c = 5A(y_0 + y_c)^{3/2}/8 \quad Ay_0^{1/2} > 2\sqrt{2}/5 \\ FC1 : \quad & y = 1 \quad A(1 + y_0)^{3/2} > 8/5, \end{aligned} \tag{4.5}$$

where  $AFC2$ ,  $CC2$ ,  $CC1$  and  $FC1$  stand for antiferromagnetic two band conducting, canted two band conducting, canted one band conducting and ferromagnetic one band conducting

respectively. Notice that  $AF$  and canted phases do not compete among them, but only with the  $F$  phase. The curves providing the boundary between the different phases are given by

$$\begin{aligned}
AFC2 - FC1 : \quad & A[(1 + y_0)^{5/2} - 2y_0^{5/2}] = 2 & 0 < y_0 < 0.127195 \\
AFC2 - CC2 : \quad & Ay_0^{1/2} = 8/15 & 0.127195 < y_0 < 1 \\
CC2 - FC1 : \quad & 5A(y_2^2 + 3y_0^2)/4 = (y_0 + y_2)^{3/2} + (y_0 - y_2)^{3/2} & 0.127195 < y_0 < 0.168457 \\
CC2 - CC1 : \quad & Ay_0^{1/2} = 2\sqrt{2}/5 & 0.168457 < y_0 < 1 \\
CC1 - FC1 : \quad & 5A(y_0 + y_1)^{3/2}/8 = y_1 & 0.168457 < y_0 < 0.5 \\
CC1 - FC1 : \quad & 5A(1 + y_0)^{3/2}/8 = 1 & 0.5 < y_0 < 1,
\end{aligned} \tag{4.6}$$

where  $y_1$  and  $y_2$  are given implicitly by the equations

$$\begin{aligned}
& [(1 + y_0)^{5/2} - (y_0 + y_2)^{5/2} - (y_0 - y_2)^{5/2}][(y_0 + y_2)^{3/2} + (y_0 - y_2)^{3/2}] = \frac{5}{2}(1 - y_2^2)(y_2^2 + 3y_0^2) \\
& (y_1 + y_0)^{5/2} + 2(1 + y_0)^{1/2}(y_1 + y_0)^2 + 3(1 - y_0)(y_1 + y_0)^{3/2} \\
& + 4(1 - 2y_0)(1 + y_0)^{1/2}(y_1 + y_0) - 8y_0(1 + y_0)(y_1 + y_0)^{1/2} - 4y_0(1 + y_0)^{3/2} = 0.
\end{aligned} \tag{4.7}$$

The outcome is plotted in fig. 1.

Recall that fig. 1 actually does not plot a phase diagram against doping but against  $y_0$  which is related to the chemical potential rather than to the number of conducting fermions or doping. Recall also that  $V_{eff}$  is to be regarded as a (zero temperature) grand canonical potential rather than as a free energy. The doping is introduced via

$$x = -a^3 \frac{\partial V_{eff}}{\partial \mu} = -\frac{a^3}{t} \frac{\partial V_{eff}}{\partial y_0} \tag{4.8}$$

provided that one molecule exists per unit cell with a lattice parameter  $a$ . Taking into account (3.9) the doping corresponding to the different phases reads

$$\begin{aligned}
AFI : \quad x &= 0 \\
AFC2 : \quad x &= \frac{z^{3/2}}{6\pi^2} 2y_0^{3/2} \\
CC2 : \quad x &= \frac{z^{3/2}}{6\pi^2} [(y_0 + y_c)^{3/2} + (y_0 - y_c)^{3/2}] \\
CC1 : \quad x &= \frac{z^{3/2}}{6\pi^2} (y_0 + y_c)^{3/2} \\
FC1 : \quad x &= \frac{z^{3/2}}{6\pi^2} (1 + y_0)^{3/2}.
\end{aligned} \tag{4.9}$$

where the  $y_c$  for the  $CC2$  and  $CC1$  phases are given in (4.5).



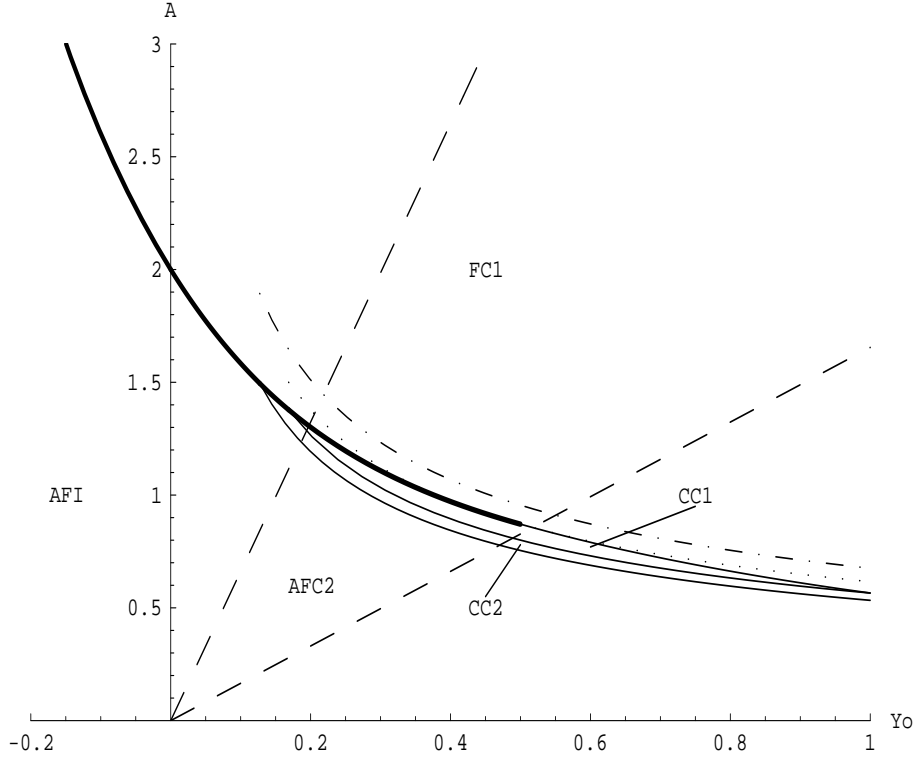


**Figure 1.** Phase diagram in the  $(y_0, A)$  plane. The thick solid line corresponds to first order transitions whereas the remaining solid lines to second order ones. The dotted and dashed dotted lines are the upper stability boundaries for the CC1 and CC2 phases respectively. The two dashed lines are the boundaries for the reliability of our model for  $z|J_H|M/2(J_A F a^3 M^2) \sim 50$  and  $z|J_H|M/2(J_A F a^3 M^2) \sim 200$  respectively. Only the part of the phase diagram to the left of the corresponding dashed line is trustworthy in each case.

These expressions for the doping permit us to establish that all our phases are thermodynamically stable, unlike the ones observed in ref. [3, 4]. This is easily proven from the stability condition  $\partial\mu/\partial x > 0$ . For the  $F$  and  $AF$  phases this is trivially obtained, whereas canted phases are stable if they are below the curves

$$\begin{aligned}
 CC2 : \quad 5Ay/3 &= (y_0 + y)^{1/2} - (y_0 - y)^{1/2} \\
 y^2 - 5y_0^2 + 4y_0(y_0^2 - y^2)^{1/2} &= 0 \quad (y < y_0) \\
 CC1 : \quad Ay_0^{1/2} &= 16/15\sqrt{3}.
 \end{aligned} \tag{4.10}$$

This is always the case as it is shown in fig. 1 where we have plotted the two curves.

Once we have the expressions (4.9) for the doping it is straightforward to translate fig. 1 to a more conventional phase diagram where the doping,  $x$ , appears in one of the axes. This is given in fig. 2 (recall  $z = 6$ ).

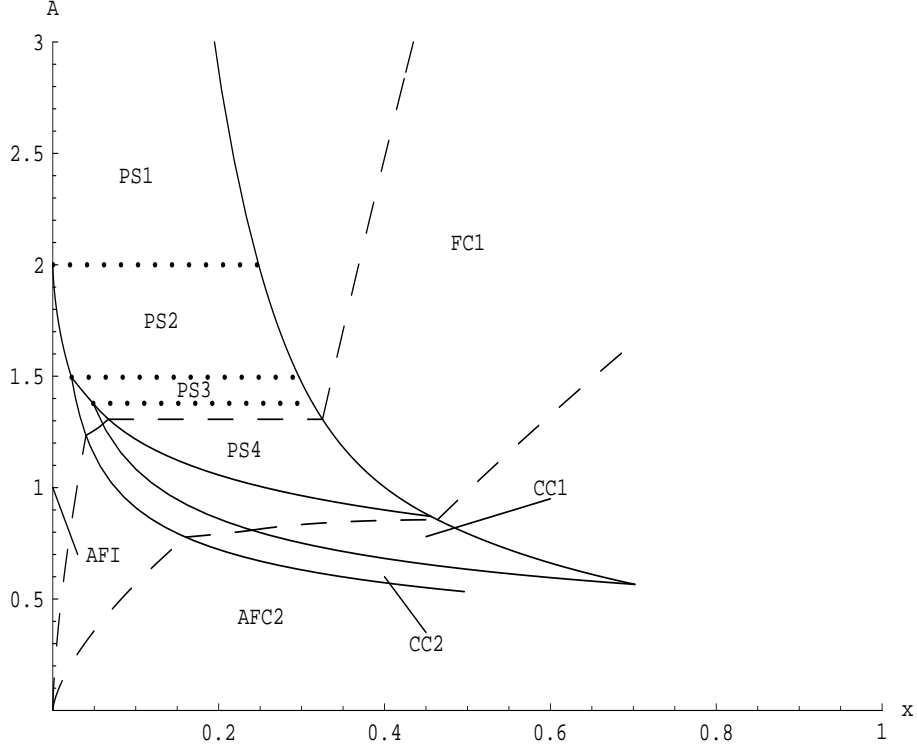


**Figure 2.** Phase diagram in the  $(x, A)$  plane.  $PSi$  ( $i = 1, 2, 3, 4$ ) indicates the new regions where the phases at their boundary may coexist. The  $x = 0$  axis corresponds to the *AFI* phase. The two dashed lines are the boundaries for the reliability of our model for  $z|J_H|M/2(J_{AF}a^3M^2) \sim 50$  and  $z|J_H|M/2(J_{AF}a^3M^2) \sim 200$  respectively. Only the part of the phase diagram to the left of the corresponding dashed line is trustworthy in each case.

It is interesting to notice that in fig. 2 new regions arise, which we have denoted  $PSi$  ( $i = 1, 2, 3, 4$ ), between the *FC1* and the *AFI*, *AFC2*, *CC2* and *CC1* phases respectively. This is due to the fact that the thick solid line separating *FC1* and *AFI*, *AFC2*, *CC2* and *CC1* in fig. 1 corresponds to a first order phase transition. Along this line two stable inequivalent minima have the same energy and the chemical potential cannot be traded by the doping. These regions are likely to consist of coexisting domains where the two phases at the boundary are realised (phase separation) [9]. *AFI* and *FC1* would coexist in *PS1*, as it has been observed in recent works [3, 4]. *FC1* and *AFC2*, *CC2* and *CC1* would coexist in *PS1*, *PS2* and *PS3* respectively. These three last possibilities of phase separation have not been found before.

As mentioned in section 3, the fact that for  $t = 0$  we do not permit conductivity restricts the values that the chemical potential takes to  $y_0 < y_0^{max} = \gamma/2$ . By substituting this

expression in  $A$  we obtain

$$A = \frac{2z^{1/2}}{15\pi^2} \frac{z|J_H|M}{2(J_{AF}a^3M^2)} y_0^{max}. \quad (4.11)$$

which gives the boundary of validity for our results. It turns out to be a straight line in fig. 1 provided that  $J_{AF}$  and  $J_H$  remains constant as  $y_0^{max}$  moves, which can be straightforwardly translated to fig. 2. Only the phase diagram to the left of this curve is trustworthy.

We take for the coupling constants  $t/(J_{AF}a^3M^2) \sim 10 - 20$  and  $z|J_H|M/2(J_{AF}a^3M^2) \sim 50 - 200$ , which is compatible with the values given in the literature. For these values  $A \sim 1 - 2$ , and the two extreme validity curves are displayed as dashed lines in fig. 1 and fig. 2.

## 5 Conclusions

We have presented a simple model in the continuum which is able to describe the rich phase structure of doped manganites for a wide range of these materials.

We have assumed an underlying cubic crystal for simplicity. Nevertheless, the orthorhombic distortion can be easily accommodated by the following simple changes in the physical parameters:  $m^3 \rightarrow m_x m_y m_z$ ,  $a^3 \rightarrow abc$ ,  $J_{AF} \rightarrow J_x + J_y + J_z$  and  $t \rightarrow t_x + t_y + t_z$ . In practice this does not modify our results since it would only lead to a different  $A$ , which is anyway a free parameter in our phase diagrams. This fact also suggests that the structural transitions that these materials undergo when increasing the doping [14] are not essential in order to understand the  $F - AF$  and  $I - C$  transitions.

An important feature of our results is that the two canted phases that we observe are stable against phase separation, unlike in some previous works [3, 4]. We also observe regions in the phase diagram where phase separations of several kinds may occur. If we plug realistic values for the physical parameters we find  $A \sim 1 - 2$ . Within this range the following sequences of phases are possible upon increasing  $x$ : (i)  $AFI - PS1 - FC1$ , (ii)  $AFI - AFC2 - PS2 - FC1$ , (iii)  $AFI - AFC2 - CC2 - PS3 - FC1$ , (iv)  $AFI - AFC2 - CC2 - CC1 - PS4 - FC1$ . Recall also that in  $PS3$  and  $PS4$  ferromagnetic and canted phases coexist, which is a situation that has not been contemplated in previous works. This may explain some controversial results obtained by different authors.

Let us also mention that the two fermion fields  $\psi_1(x)$  and  $\psi_2(x)$  accommodate the  $e_g$  doublet in our model. Indeed in the  $AF$  phase the two lower and two higher eigenvalues (3.4) are degenerated. In the  $F$  and  $C$  phases the degeneracy is lifted. This implies that the splitting between the two  $e_g$  levels receives a contribution from the dynamics of the conducting fermions in addition to that from the static Jahn-Teller distortion.

The model can be used in the future to study the temperature dependence of the phase diagram. Fluctuations due to spin waves in all the phases (including the canted ones) can also be incorporated [16]. It would also be interesting to see if the model can be generalised to accommodate the Jahn-Teller distortion dynamically.

## Acknowledgements

We are indebted to F. Guinea and L. Brey for introducing us to the physics of manganites, and to J. González for an illuminating discussion in the early stages of this work. J.M.R is supported by a Basque Government F.P.I. grant. Financial support from CICYT, contract AEN95-0590 and from CIRIT, contract GRQ93-1047 is also acknowledged.

## Appendix A: $\zeta$ -function Techniques

The  $\zeta$ -function techniques provide a very efficient way to calculate the trace of the logarithm of operators [15]. The  $\zeta$ -function associated to an operator  $\hat{O}$  is defined as

$$\zeta_{\hat{O}}(s) := \text{tr} \hat{O}^{-s} = \sum_n \lambda_n^{-s}. \quad (\text{A.1})$$

Then

$$\sum_n \log \lambda_n = - \left. \frac{d}{ds} \zeta_{\hat{O}}(s) \right|_{s=0}. \quad (\text{A.2})$$

Consider the operator  $\hat{O}$  in (3.2). Once the spin diagonalisation is performed we only have to consider the space-time trace over a generic spin eigenvalue denoted by  $\hat{O}_i$ . Since the real part of the operator  $-i\hat{O}_i$  is positive for positive energies and negative for negative ones, due to the term  $i\epsilon\omega$  in (3.4), it is convenient to consider the integral form of  $\zeta_{\hat{O}}(s)$  over positive and negative energies of separately.

$$\text{tr}[(\hat{O}_i \theta(-\omega))^{-s}] = \frac{(-i)^{-s}}{\Gamma(s)} \int_0^\infty d\tau \tau^{s-1} \int_{-\infty}^0 \frac{dw}{2\pi} \frac{d^3 \mathbf{k}}{(2\pi)^3} e^{-iO_i(q)\tau} VT \quad (\text{A.3a})$$

$$\text{tr}[(\hat{O}_i \theta(\omega))^{-s}] = \frac{i^{-s}}{\Gamma(s)} \int_0^\infty d\tau \tau^{s-1} \int_0^\infty \frac{dw}{2\pi} \frac{d^3 \mathbf{k}}{(2\pi)^3} e^{iO_i(q)\tau} VT. \quad (\text{A.3b})$$

After the energy and momentum integration we obtain the expressions

$$\text{tr}[(\hat{O}_i \theta(-\omega))^{-s}] = \frac{VT}{16\pi} \left( \frac{2m}{\pi} \right)^{3/2} \frac{\Gamma(s-5/2)}{\Gamma(s)} (-i)^{-s-5/2} (-i\Omega_i)^{s+5/2} \quad (\text{A.4a})$$

$$\text{tr}[(\hat{O}_i \theta(\omega))^{-s}] = -\frac{VT}{16\pi} \left( \frac{2m}{\pi} \right)^{3/2} \frac{\Gamma(s-5/2)}{\Gamma(s)} (-i)^{s+5/2} (i\Omega_i)^{-s+5/2}. \quad (\text{A.4b})$$

We need the derivative of the above with respect to  $s$  at  $s = 0$ . The presence of  $1/\Gamma(s) \sim s$  makes the evaluation very easy, giving rise to

$$-\frac{d}{ds} \zeta_{\hat{O}}(s) \Big|_{s=0} = \frac{VT(2m)^{3/2}}{30\pi^2} \left[ i^{5/2}(-i\Omega_i)^{5/2} - (-i)^{5/2}(i\Omega_i)^{5/2} \right]. \quad (\text{A.5})$$

The expression between square brackets vanishes when  $\Omega_i > 0$ , i.e., when the chemical potential is below the energy of the  $i$ -th state, and is non zero when  $\Omega_i < 0$ , i.e., when the chemical potential is above the energy of the  $i$ -th state. This leads to the effective potential (for  $\mu < 0$ ,  $y_0 < y_0^{max} < 1$ )

$$V_{eff} = V_0 \left[ (2y^2 - 1) - \frac{A}{\gamma^{5/2}} \left[ \left( \sqrt{1 + \frac{2\gamma y}{1 + \gamma^2}} - \sqrt{1 - \frac{2\gamma y_0}{1 + \gamma^2}} \right)^{5/2} \theta(y_0 + y) + \left( \sqrt{1 - \frac{2\gamma y}{1 + \gamma^2}} - \sqrt{1 - \frac{2\gamma y_0}{1 + \gamma^2}} \right)^{5/2} \theta(y_0 - y) \right] \right], \quad (\text{A.6})$$

where  $y = \cos(\theta/2)$ , whereas  $\gamma$ ,  $y_0$ , and  $V_0$  are defined in (3.5), (3.6) and (3.9) respectively.

$$A = \frac{(2m)^{3/2}}{15\pi^2 J_{AF} M^2} \left( t \sqrt{1 + \gamma^2} \right)^{5/2}. \quad (\text{A.7})$$

Eq. (3.7) follows from the above by keeping only terms linear in  $\gamma$ .

## References

- [1] G. H. Jonker and J. H. Van Santen, *Physica* **50** (1950) 337.
- [2] D. P. Arovas and F. Guinea, *Phase Diagram of Doped Manganates*, cond-mat/9711145.
- [3] D. P. Arovas, G. Gómez-Santos and F. Guinea, *Phase Separation in Double Exchange Systems*, cond-mat/9805399.
- [4] M. Yu Kagan, D. I. Khomskii and M. Mostovoy, *Canted Spin or Phase Separation in the Double-Exchange Model*, cond-mat/9804213.
- [5] L.-J. Zou, Q.-Q. Zheng and H. Q. Liu, *Phys. Rev.* **B56** (1997) 13669.
- [6] A. J. Millis, P. B. Littlewood and B. I. Shraiman, *Phys. Rev. Lett.* **75** (1995) 5144.
- [7] R. Maezono, S. Ishihara and N. Nagaosa, *Phase Diagram in Manganese Oxides*, cond-mat/9805267.

- [8] D. I. Golosov, M. R. Norman and K. Levin, *On the Theory of Magnets with Competing Double Exchange and Superexchange Interactions*, cond-mat/9805238.
- [9] S. Yunoki, A. Moreo and E. Dagotto, *Phase Separation Induced by Orbital Degrees of Freedom in Models for Manganites with Jahn-Teller Phonons*, cond-mat/9807149.  
 E. Dagotto, S. Yunoki and A. Moreo, *Phase separation in models for manganites: theoretical aspects and comparison with experiments*, cond-mat/9809380.
- [10] J. W. Lynn *et al.*, *Phys. Rev. Lett.* **76** (1996) 4046;  
 Y. Yamada *et al.*, *Phys. Rev. Lett.* **77** (1996) 904;  
 G. Allodi *et al.*, *Phys. Rev.* **B56** (1997) 6036;  
 J. M. De Teresa *et al.*, *Phys. Rev.* **B57** (1998) 3305;  
 M. Hennion *et al.*, cond-mat/9806272;  
 Wei Bao *et al.*, *Solid State Comm.* **98** (1996) 55.
- [11] C. Zener, *Phys. Rev.* **82** (1951) 403.
- [12] P. W. Anderson and H. Hasegawa, *Phys. Rev.* **100** (1955) 675.
- [13] P. G. De Gennes *Phys. Rev.* **118** (1960) 141.
- [14] A. P. Ramirez, *J. Phys.: Cond. Matter* **9** (1997) 8171.
- [15] E. Elizalde *et al.*, *Zeta Regularization Techniques with Applications*, (World Scientific Cop., Singapore, 1994).
- [16] J.M. Román and J. Soto, *Spin Waves in Canted Phases*, in preparation, preprint no. UB-ECM-PF 98/19.